The Capacity-Maximizing Field of View of an Optical Communications System

Bruce Moision*

ABSTRACT. — We address the problem of selecting an optimum field of view (FOV) for an optical communications link. We derive a closed-form equation that provides an approximation to the optimum FOV as a function of an incident signal-to-noise-ratio (SNR_i) and the signal spot intensity variance. Using this expression, we show that in the limit of small SNR_i one wants to encircle 72 percent of the signal power. The optimum fraction is increasing with SNR_i, so it follows that one always wants to encircle at least 72 percent of the signal. We provide an expression for the loss in selecting a suboptimal FOV and find the FOV that we conjecture minimizes the maximum loss. This FOV corresponds to encircling 91 percent of the signal power and limits the maximum loss to less than 0.4 dB in signal power for a target capacity. Finally, we illustrate an application of using the estimate to select an optimum FOV for a pixellated focal plane illuminated by a speckled signal intensity pattern.

I. Introduction

In a free-space optical communications system, one may utilize an iris to adjust the field of view (FOV). Reducing the FOV has the effect of filtering out both background noise and signal power. The optimum setting of the FOV may be taken to be the value that maximizes the channel capacity. This optimum depends on the magnitude of the signal power, the spatial distribution of the signal power in the focal plane, and the intensity of the noise power. In this article, we derive a simple approximation to the optimum FOV for an intensity-modulated, direct-detected, pulse-position-modulation (PPM) communications link. Using the approximation, we show that one should always encircle at least 72 percent of the signal power, and illustrate the loss due to choosing a suboptimum FOV. We show that if one were to encircle 91 percent of the signal power for all signal and noise pairs, the loss, relative to the optimum setting, is less than 0.4 dB, and we conjecture this represents the minimum worst-case loss for a fixed FOV.

* Communications Architectures and Research Section.

The research described in this publication was carried out by the Jet Propulsion Laboratory, California Institute of Technology, under a contract with the National Aeronautics and Space Administration.

II. Channel Model

A simple model of the receiver is illustrated in Figure 1. We put

D = aperture diameter (m),
F = focal length (m),
r_0 = atmospheric coherence length (Fried parameter) (m),
I_s = incident signal irradiance (W/m^2),
I_b = incident background spectral radiance (W/m^2/μm/sr),
Ω = detector field of view (sr),
λ = wavelength (m), and
δ = effective detector radius (m).

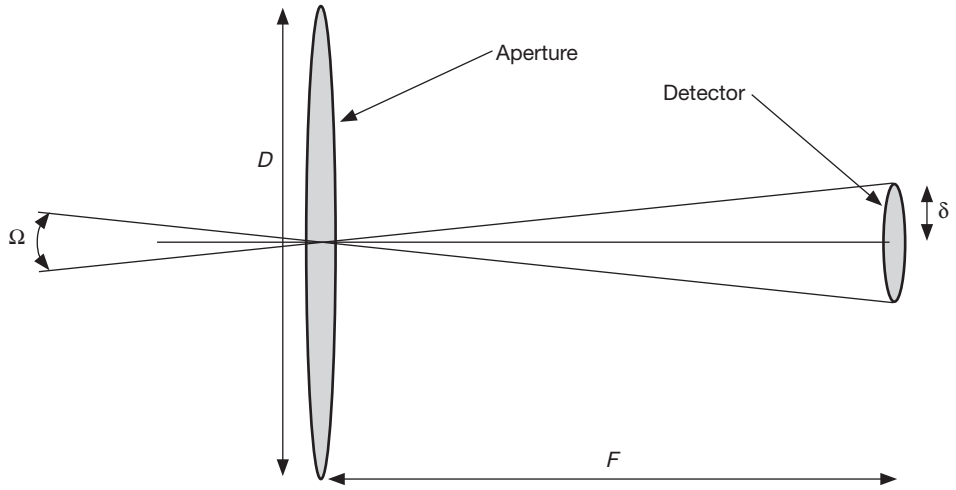

Figure 1. Free-space optical receiver.

We assume the telescope and channel parameters ($D, F, r_0, I_s, I_b, \lambda$) are fixed, and that the operator may adjust the FOV by changing δ with an adjustable iris (this could also be accomplished via signal processing if we replace a single detector with an array, an approach we describe in Section V). Let $I(x,y)$ be the normalized mean signal intensity function in the focal plane, such that

$$\int_{\mathcal{A}} I(x,y)\, dxdy$$

is the fraction of the signal incident on an area $\mathcal{A}$. We assume that the mean signal intensity may be modeled as Gaussian

$$I(x,y) = \frac{1}{2\pi\sigma^2} \exp\left(\frac{-(x^2+y^2)}{2\sigma^2}\right) \tag{1}$$

where

$$\sigma = \left(0.42\lambda F\right)\sqrt{\left(\frac{1}{r_0}\right)^2 + \left(\frac{1}{D}\right)^2}$$

This reduces to a diffraction-limited spot when $r_0 \gg D$, and corresponds to the turbulence-limited mean spot size when $D \gg r_0$, which is significantly larger than the diffraction-limited spot size, representing the blurring of the spot in turbulence. For the purpose of deriving an optimum FOV, we presume the intensity is fixed in time, and given by this long-term average. Although the intensity is a random process, we find that an analysis based on Equation (1) provides results that are sufficiently accurate for our purposes. In Section V, we will illustrate the accuracy of the approximation when applied to predicting the behavior of a short-term intensity (speckle) pattern.

Let I_s be the signal irradiance, η be the system efficiency (the fraction of photons incident on the aperture that are converted to photo-electrons), $E_\lambda = hc/\lambda$, the energy per photon, and

$$K_s = \frac{I_s \eta \pi D^2}{4E_\lambda} \text{ pe/s}$$

the total signal photo-electron (pe) flux that would be collected in the focal plane with an infinite-area photodetector (in the absence of an iris). Let l_s denote total signal flux collected by the photodetector with an iris of radius δ present. We have

$$\begin{aligned} l_s &= K_s \int_{\mathcal{A}(\delta)} I(x,y)\, dxdy \\ &= K_s \int_{\theta=0}^{2\pi} \int_{r=0}^{\delta} \frac{r}{2\pi\sigma^2} \exp\left(\frac{-r^2}{2\sigma^2}\right) drd\theta \\ &= K_s \left(1 - e^{-\delta^2/2\sigma^2}\right) \end{aligned}$$

Let l_n denote the aggregate noise pe flux rate. We assume this is dominated by sky radiance, and is given by [1]:

$$l_n = \frac{I_b \eta \pi D^2 \Omega \Delta_\lambda}{4E_\lambda}$$

where Δ_λ is the bandwidth of a narrow-band filter and Ω is the solid angle subtended by the photodetector relative to the aperture center. Assuming small angles, we put

$$\Omega \approx \pi \left(\frac{\delta}{F}\right)^2$$

and, for our purposes, write l_n as

$$l_n = K_n \pi \delta^2$$

where

$$K_n \stackrel{\text{def}}{=} \frac{\pi D^2 \Delta_\lambda I_b \eta}{4E_\lambda F^2}$$

is the aggregate noise pe spatial flux density, in pe/s/m^2. We also define two notions of the signal-to-noise ratio (SNR) of the system. Let

$$\mathrm{SNR} \stackrel{\mathrm{def}}{=} \frac{l_S(M-1)}{l_n 2\ln(M)}$$

$$\mathrm{SNR}_i \stackrel{\mathrm{def}}{=} \frac{K_S}{K_n \pi(2\sigma)^2} \frac{(M-1)}{2\ln(M)}$$

The first term, SNR, is the achieved ratio of signal-to-noise rates, after spatial filtering with the iris, scaled by $(M-1)/(2\ln(M))$, to account for how the PPM order impacts the mapping of signal and noise rates to the capacity. The second term, SNR_i, reflects the *incident*, or *initial*, ratio of signal and noise rates, prior to spatial filtering. It is the ratio of the total signal pe rate to the total noise pe-rate collected in an area with radius 2σ — the area that would correspond to collecting 86.5 percent of the signal power. We will see later that 86.5 percent roughly corresponds to a notion of a nominal optimum collecting area.

III. Capacity-Maximizing Field of View

We presume we are signaling with PPM of order M, and that the photo-electron point processes are well modeled as Poisson. The capacity of this Poisson PPM channel is not known in a form that facilitates a tractable analysis. However, it may be approximated as [2]:

$$C \approx \frac{l_s}{\ln(2)\left(\frac{1}{\ln(M)} + \frac{2}{M-1}\frac{l_n}{l_s}\right)} \text{ bits/s} \tag{2}$$

In Sections III and IV, we presume Equation (2) holds with equality. In Section V, we compare the predictions made using this approximation to an exact (numerical) computation of the capacity, illustrating the accuracy of using Equation (2).

Setting the derivative of Equation (2) with respect to δ to zero yields

$$l_s'\left(\frac{M-1}{2\ln(M)} + \frac{2l_n}{l_s}\right) - l_n' = 0 \tag{3}$$

where

$$l_s' = \frac{\partial l_s}{\partial \delta} = K_s \frac{\delta}{\sigma^2} e^{-\delta^2/2\sigma^2}$$

$$l_n' = \frac{\partial l_n}{\partial \delta} = K_n 2\pi\delta$$

Substitution into Equation (3) yields

$$\frac{K_s e^{-\delta^2/2\sigma^2}\delta}{\sigma^2}\left(\frac{(M-1)}{2\ln(M)} + \frac{2\pi\delta^2 K_n}{K_s(1-e^{-\delta^2/2\sigma^2})}\right) - 2\pi\delta K_n = 0 \tag{4}$$

Putting

$$\gamma \stackrel{\text{def}}{=} \frac{\delta^2}{2\sigma^2}$$

we may rewrite Equation (4) as

$$2\,\mathrm{SNR}_i + \frac{2\gamma}{1 - e^{-\gamma}} - e^{\gamma} = 0 \tag{5}$$

This relates the optimum value of δ in terms of the incident signal-to-noise ratio, SNR_i, and the spot width (as $\gamma = \delta^2/2\sigma^2$). Figure 2 illustrates the resulting fraction of the signal power, $(1 - e^{-\gamma})$, encircled by the optimum δ. As SNR_i increases, one wants to encircle more signal power. In the limit of large SNR_i, one wants to collect all of the signal. As SNR_i decreases, the cost of collecting the tails of the spot increases, and one wants to encircle less of the spot. In the limit of small SNR_i, we have

$$\gamma = \gamma^*_{\text{min}} \stackrel{\text{def}}{=} 1.2564$$

corresponding to collecting 71.53 percent of the signal power. Finally, we note that larger PPM orders makes one more resilient to noise, as is seen in Equation (2).

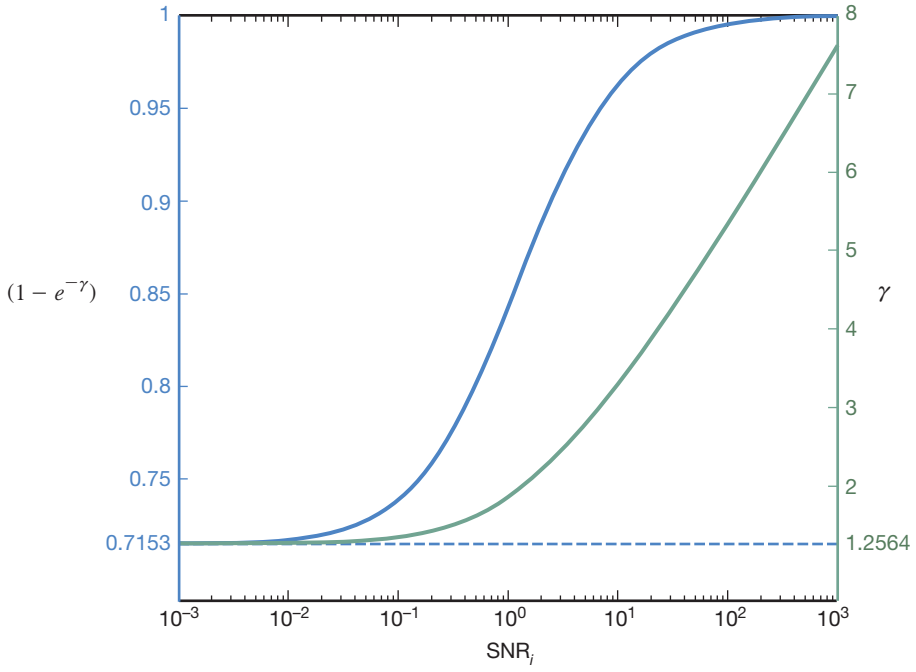

Figure 2. Optimum fraction of encircled signal power $(1 - e^{-\gamma})$ and FOV parameter γ as a function of SNR_i.

IV. Cost of a Suboptimal Field of View

Suppose one selects a suboptimal FOV. What loss is incurred in this choice? And is there a FOV, specified by a fixed γ, that minimizes that loss? In this section, we address these questions.

Fix K_n, M, and σ. Select a signal rate K_s^*. Let SNR_i^* be the corresponding input SNR, γ^* the optimum FOV parameter, satisfying Equation (5), SNR^* the corresponding achieved SNR, and C the achieved capacity. Now suppose, for the same K_n, M, and σ, one desires to achieve the same capacity C, but selects a suboptimum $\gamma \neq \gamma^*$. Let K_s denote the signal rate required to achieve capacity C with this selection of γ, and SNR the corresponding SNR. Since the capacity is monotonic in the signal rate, and K_s^* is the minimum rate to achieve C, we must have $K_s > K_s^*$. The ratio K_s/K_s^* then represents the increase in signal power, or loss, due to the suboptimal choice of γ. How large can this be, and how can it be minimized?

Using Equation (2) and setting the capacity of the two cases equal yields

$$\frac{K_s(1-e^{-\gamma})}{1+\frac{1}{\mathrm{SNR}}} = \frac{K_s^*(1-e^{-\gamma^*})}{1+\frac{1}{\mathrm{SNR}^*}}$$

Substituting $\mathrm{SNR} = 2K_s(1-e^{\gamma})(M-1)/(2\ln(M)\pi(2\sigma^2)K_n\gamma)$, we obtain a quadratic in K_s, which may be factored to yield

$$\frac{K_s}{K_s^*} = \frac{\left(1-e^{-\gamma^*}\right)}{\left(1-e^{-\gamma}\right)}\left(\frac{1+\sqrt{1+4\frac{\gamma}{\gamma^*}\frac{1}{\mathrm{SNR}^*}\left(1+\frac{1}{\mathrm{SNR}^*}\right)}}{2\left(1+\frac{1}{\mathrm{SNR}^*}\right)}\right) \tag{6}$$

Figure 3 illustrates losses given by Equation (6) as a function of SNR_i for a range of values of γ. As one would expect, the loss, from Equation (6), is unbounded in the limits $\gamma \to 0$ and $\gamma \to \infty$. We would like to know, for a nonzero, finite, choice of γ, what is the worst-case loss? For $\gamma \leq \gamma^*$, we have

$$\begin{aligned}\frac{K_s}{K_s^*} &\leq \frac{\left(1-e^{-\gamma^*}\right)}{\left(1-e^{-\gamma}\right)}\left(\frac{1+\sqrt{1+\frac{4}{\mathrm{SNR}^*}\left(1+\frac{1}{\mathrm{SNR}^*}\right)}}{2\left(1+\frac{1}{\mathrm{SNR}^*}\right)}\right)\\ &= \frac{\left(1-e^{-\gamma^*}\right)}{\left(1-e^{-\gamma}\right)}\\ &\leq \frac{1}{\left(1-e^{-\gamma}\right)}\end{aligned} \tag{7}$$

We can see this, intuitively, as follows. When $\gamma < \gamma^*$, we are encircling a smaller fraction of the signal, and less noise. In the worst case, the noise is negligible, so there is no gain from filtering out noise, and we must increase K_s to compensate for the smaller encircled fraction, that is, we have $K_s(1-e^{-\gamma}) = K_s^*(1-e^{-\gamma^*})$.

For $\gamma > \gamma^*$, we have

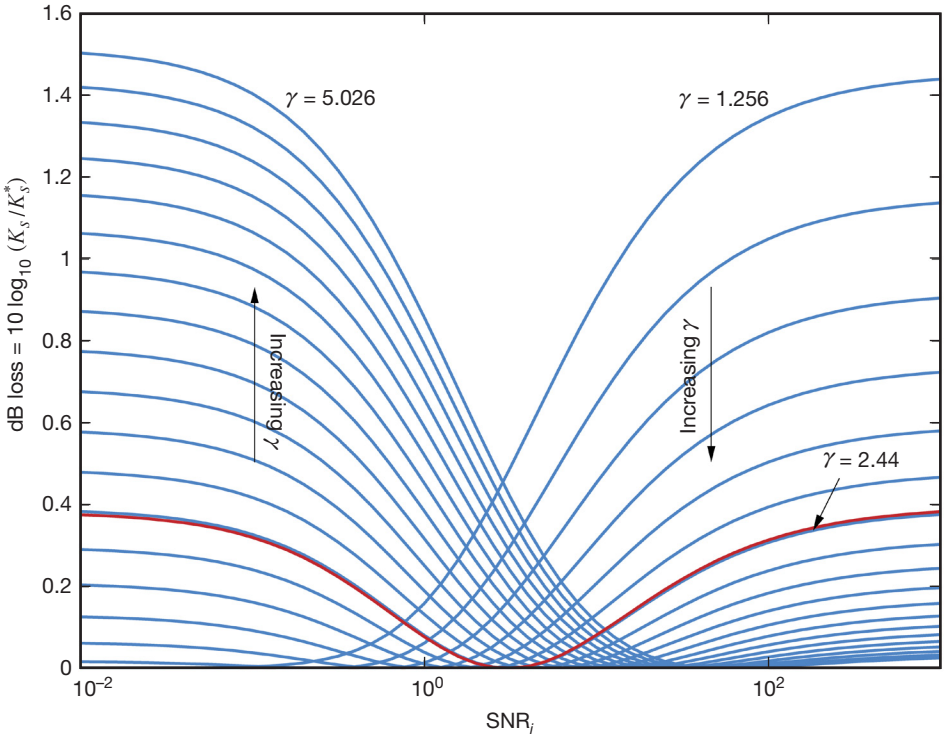

Figure 3. Loss due to suboptimal FOV as a function of SNR_i. Each curve parameterized by fixed γ. The red curve corresponds to γ = 2.44, which corresponds to the FOV that minimizes the maximum loss.

$$\begin{aligned}\frac{K_s}{K_s^*} &= \frac{\left(1-e^{-\gamma^*}\right)}{\left(1-e^{-\gamma}\right)}\left(\sqrt{\frac{\gamma}{\gamma^*}}\frac{\sqrt{\frac{\gamma^*}{\gamma}}+\sqrt{\frac{\gamma^*}{\gamma}+\frac{4}{\mathrm{SNR}^*}\left(1+\frac{1}{\mathrm{SNR}^*}\right)}}{2\left(1+\frac{1}{\mathrm{SNR}^*}\right)}\right)\\ &\le \frac{\left(1-e^{-\gamma^*}\right)}{\left(1-e^{-\gamma}\right)}\sqrt{\frac{\gamma}{\gamma^*}}\left(\frac{1+\sqrt{1+4\frac{1}{\mathrm{SNR}^*}\left(1+\frac{1}{\mathrm{SNR}^*}\right)}}{2\left(1+\frac{4}{\mathrm{SNR}^*}\right)}\right)\\ &= \frac{\left(1-e^{-\gamma^*}\right)}{\left(1-e^{-\gamma}\right)}\sqrt{\frac{\gamma}{\gamma^*}}\\ &\le 0.64\frac{\sqrt{\gamma}}{\left(1-e^{-\gamma}\right)}\end{aligned} \tag{8}$$

where, in Equation (8) we use the fact that $\gamma^*_{\mathrm{min}} = 1.2564$ maximizes $(1-e^{-\gamma^*})/\sqrt{\gamma^*}$. In this case, when $\gamma > \gamma^*$, we are encircling more noise than is optimal. The greatest penalty for this additional noise occurs when we are in the noise-dominated regime, where the capacity goes as l_s^2/l_b. Since the noise is presumed uniform, the ratio γ/γ^* is the increase in total noise flux. To offset this increase in noise flux, the total encircled signal power must be increased by the square of the ratio times the ratio of the encircled signal.

Note that the worst-case losses, Equations (7) and (8), correspond to the limits of small and large SNR_i (equivalently, small and large SNR^* or γ^*, respectively. That is, the largest loss for a fixed γ occurs either for $\gamma^* = \gamma^*_{\mathrm{min}}$ or for $\gamma^* \to \infty$. Suppose one wants to choose γ for a system to minimize the maximum loss. Setting the maximum losses given by Equations (8) and (7), equal and solving for γ yields

$$\gamma = 2.44$$

The curve corresponding to this γ is illustrated in Figure 3. This corresponds to encircling 91.3 percent of the signal power, and yields a worst-case loss of 0.4 dB. Hence, if one were to always choose to encircle 91.3 percent of the signal, the loss would be no greater than 0.4 dB relative to the optimum FOV.

V. Example: Application to a Pixellated Focal Plane

In this section, we provide an example to illustrate the accuracy of the (approximate) optimum given by Equation (5) when we remove several approximations used to derive Equation (5). In this numerical example, we assume the focal plane is populated by an array of photodetectors and the intensity pattern is speckled, rather than approximated by the long-term average. We also utilize (a numerical estimate of) the exact capacity, rather than use Equation (2).

We assume the detectors are square, and perfectly fill the plane, with each side l meters. The system parameters, chosen from models of a deep-space downlink, are listed in Table 1. We model the speckled intensity pattern as follows.[1] Let

$$I'(x,y) = \frac{1}{N}\sum_{n=1}^{N} I_G(x - x_i, y - y_i)$$

where $N = \lceil (D/r_0)^2 \rceil$, we assume $N \gg 1$, the x_i and y_i are independent, identically distributed, zero mean, Gaussian random variables with standard deviation

$$\sigma_0 = \frac{0.42\lambda F}{r_0}$$

and

$$I_G(x,y) = \frac{1}{2\pi\sigma_G^2}\exp\left(-(x^2+y^2)/(2\sigma_G^2)\right)$$

with

$$\sigma_G = \frac{0.42\lambda F}{D}$$

This corresponds to the presence of $\lceil (D/r_0)^2 \rceil$ speckle centers, each producing a diffraction pattern I_G centered at the random offset (x_i, y_i). Note that $E[I'(x,y)] = I(x,y)$. For each realization of the set $\{(x_i, y_i)\}$, the jth detector collects a fraction

$$\int_{\mathcal{A}_j} I'(x,y)\,dxdy$$

of the signal power, where $\mathcal{A}_j$ is the area of the detector. An example for the parameters from Table 1 is illustrated in Figure 4.

[1] Sabino Piazzolla, personal correspondence, Communications Architectures and Research Section, Jet Propulsion Laboratory, Pasadena, California, 2012.

Table 1. System parameters for an example of a random speckle pattern incident on a pixellated focal plane. Optimum FOVs (indicated by the fraction of encircled signal power, $(1-e^{-\gamma})$ and the corresponding number of pixels, K) are indicated for $\mathrm{SNR}_i \in \{0.1, 1.0, 10.0, 100.0\}$. Also listed are the corresponding estimated optimum values, showing good agreement.

I_b(W/cm^2 sr μm)	4.00×10^{-4}			
Δ_λ (nm)	0.5			
r_0 (cm)	5			
D (m)	1.0			
F (m)	10.0			
l (μm)	40			
η	0.1			
M	64			
I_s(dB-W/m^2)	–135.8	–125.8	–115.8	–105.8
SNR_i	0.1	1.0	10.0	100.0
K	48	65	90	118
$(1-e^{-\gamma})$	0.78	0.87	0.94	0.98
$\hat{K}$	43	59	104	168
$(1-e^{-\hat{\gamma}})$	0.74	0.84	0.96	0.99

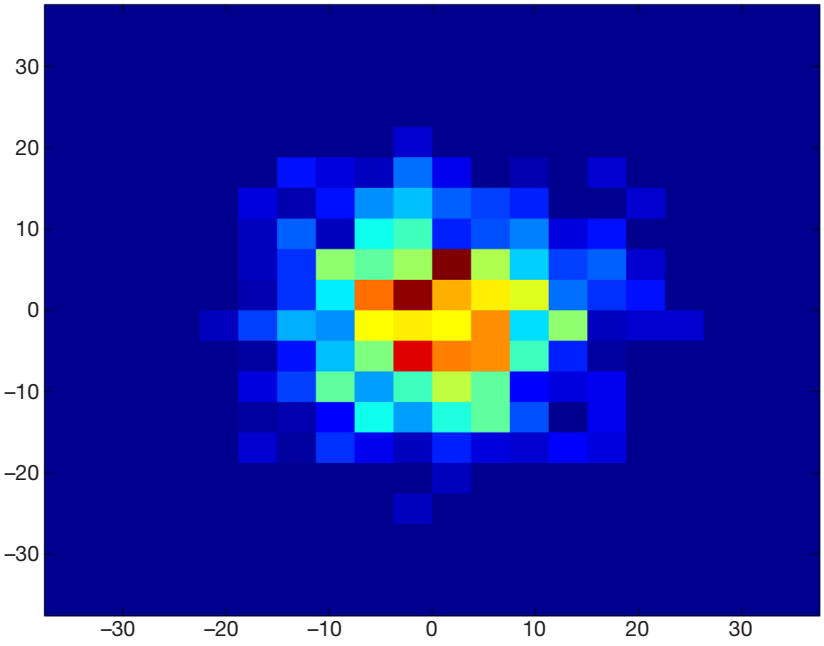

Figure 4. A randomly generated speckle pattern with parameters specified in Table 1.

To determine the optimum field of view, we put the pixels in order of their distance from the center of the intensity pattern. We evaluate the capacity achieved by summing the first (smallest distance) n pixels, $n = 1, 2, 3, \ldots$, and choose the set that returns the maximum capacity. We do not consider weighted combining, as we conjecture that a simple on-off combining will suffer only a small loss, see, e.g., [3], and is simpler to implement. We also do not consider sorting among the closest n pixels. For example, one could simply select the subset that maximizes the capacity. This provides varying gains, depending on r_0, the pixel size, and the signal and noise powers, but was not the emphasis of this work.

To evaluate the capacity, we approximate the exact bandwidth (or slotwidth) constrained expression numerically, see, e.g., [4], and select a slotwidth T_s that yields $C \approx (1/2) * \log_2(M) / (MT_s)$, corresponding to rate-1/2 redundancy. The set, in turn, specifies the optimum FOV, and fraction of encircled signal power. Each realization of the speckle pattern may yield a different optimum FOV. Table 1 lists the results, averaged over 100 realizations of the intensity pattern: the optimum number of detectors, K, and the corresponding fraction of encircled power $(1 - e^{-\gamma})$, for input $\mathrm{SNR}_i \in \{0.1, 1.0, 10.0, 100.0\}$. Also listed are the estimated optimum number of pixels, $\hat{K}$, and fraction of encircled signal power $(1 - e^{-\hat{\gamma}})$, where $\hat{\gamma}$ is chosen to satisfy Equation (5). We see that the $\hat{K}$ overestimates the optimum at large SNR_i and underestimates at small SNR_i. Figures 5 and 6 illustrate the capacity averaged over 100 realizations of the intensity pattern as functions of the number of combined pixels and the corresponding fraction of encircled signal energy, respectively, for the $\mathrm{SNR}_i = 1.0$ case from Table 1, with $T_s = 3 \times 10^{-7}$ s. In this example, we see an optimum average fraction of encircled signal power of 87 percent, and a fraction predicted by Equation (5) of 84 percent. The standard deviation on the random optimum encircled energy is 3.4 percent. The capacity function is relatively flat over a range of combined pixels around the peak, hence we can expect both some deviation in the estimate, and that the impact of that error to be small.

Acknowledgments

Many thanks to Baris Erkmen and Sabino Piazzolla for discussions on this work.

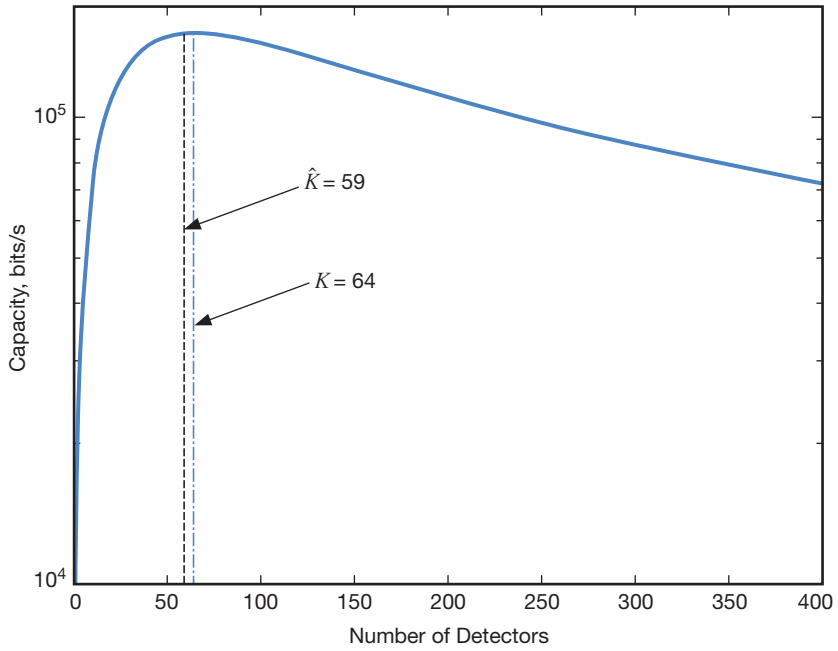

Figure 5. Capacity as a function of the average number of combined pixels, for 100 speckle patterns with parameters specified by the $\mathrm{SNR}_i = 1.0$ entry in Table 1, with slotwidth $T_s = 3.0 \times 10^{-7}$ s. The optimum number of pixels, $K = 64$, and the estimate, $\hat{K} = 59$, are illustrated.

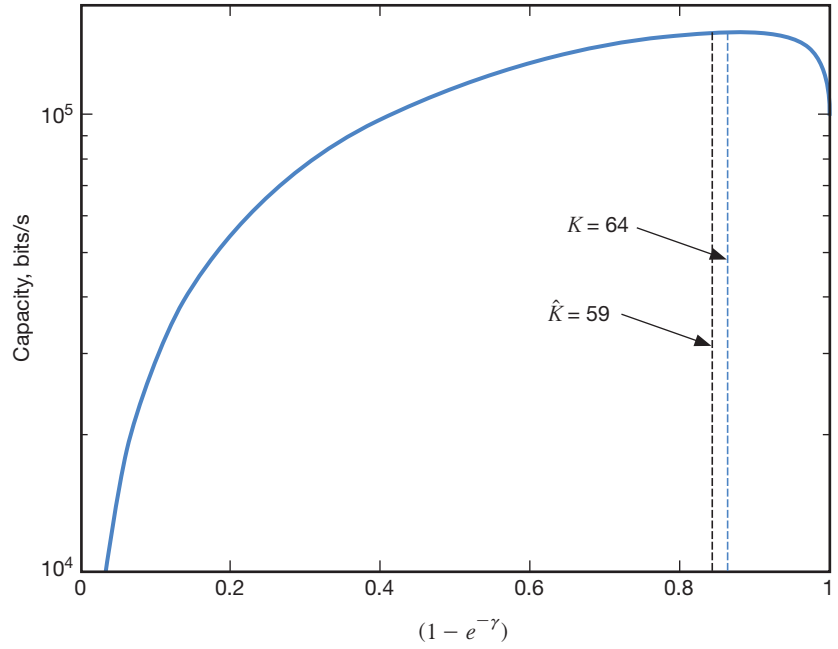

Figure 6. Capacity as a function of the average fraction of encircled power, for 100 speckle patterns with parameters specified by the $\mathrm{SNR}_i = 1.0$ entry in Table 1, with slotwidth $T_s = 3.0 \times 10^{-7}$ s. The optimum number of pixels, $K = 64$, and the estimate, $\hat{K} = 59$, are illustrated.

References

[1] A. Biswas and S. Piazzolla, "Deep-Space Optical Communications Downlink Budget from Mars: System Parameters," *The Interplanetary Network Progress Report*, vol. 42-154, Jet Propulsion Laboratory, Pasadena, California, pp. 1–38, August 15, 2003. http://ipnpr.jpl.nasa.gov/progress_report/42-154/154L.pdf

[2] B. Moision, S. Shambayati, and J. Wu, "An Optical Communications Link Design Tool for Long-Term Mission Planning for Deep-Space Missions," *Proceedings of IEEE Aerospace Conference*, Big Sky, Montana, March 3–10, 2012.

[3] V. A. Vilnrotter and M. Srinivasan, "Adaptive Detector Arrays for Optical Communications Receivers," *IEEE Transactions on Communications*, vol. 50, pp. 1091–1097, July 2002.

[4] B. Moision and J. Hamkins, "Deep-Space Optical Communications Downlink Budget: Modulation and Coding," *The Interplanetary Network Progress Report*, vol. 42-154, Jet Propulsion Laboratory, Pasadena, California, pp. 1–28, August 15, 2003. http://ipnpr.jpl.nasa.gov/progress_report/42-154/154K.pdf